

Behind-the-Meter Storage

Anthony Burrell

National Renewable Energy Laboratory
 15013 Denver West Parkway
 Golden, CO 80401
 Phone: (303) 384-6666
 E-mail: anthony.burrell@nrel.gov

Samuel Gillard, DOE-EERE-VTO

Technology Manager, Battery R&D
 Phone: (202) 287-5849
 E-mail: samuel.gillard@ee.doe.gov

Start Date: 1 October 2018

End Date: 30 September 2022

Table of Contents

	Page
Overview	1
BTMS Analysis: Financial Metrics	4
BTMS Power Electronics for Behind-the-Meter Storage	12
BTMS Testing	19
BTMS Materials Development	24

Project Introduction

This initiative, referred to as Behind-the-Meter Storage (BTMS), focuses on novel critical-materials-free battery technologies to facilitate the integration of electric vehicle (EV) charging, solar power-generation technologies, and energy-efficient buildings while minimizing both costs and grid impacts. For extreme fast-charging at levels of 350 kW or higher, novel approaches are required to avoid significant negative cost and resiliency impacts. However, it is reasonable to assume that BTMS solutions would be applicable to other intermittent renewable energy generation sources or short-duration, high-power-demand electric loads. BTMS research is targeted at developing innovative energy-storage technology specifically optimized for stationary applications below 10 MWh that will minimize the need for significant grid upgrades. Additionally, avoiding excessive high power draws will eliminate excess demand charges that would be incurred during 350-kW fast-charging using current technologies. The key to achieving this is to leverage battery-storage solutions that can discharge at high power but be recharged at standard lower power rates, acting as a power reservoir to bridge to the grid and other on-site energy-generation technologies such as solar photovoltaics (PV), thereby minimizing costs and grid impacts. To be successful, new and innovative integration treatments must be developed for seamless interaction between stationary storage, PV generation, building systems, and the electric grid.

Key components of BTMS address early-stage research into new energy-generation and building-integration concepts, critical-materials-free battery energy-storage chemistries, and energy-storage designs with a focus on

new stationary energy-storage strategies that will balance performance and costs for expanded fast-charging networks while minimizing the need for grid improvements.

Objectives

A cohesive multidisciplinary research effort is being taken to create a cost-effective, critical-materials-free solution to BTMS by employing a whole-systems approach. The focus of this initiative is to develop innovative battery energy-storage technologies with abundant materials applicable to EVs and high-power charging systems. Solutions in the 1–10 MWh range will eliminate potential grid impacts of high-power EV charging systems as well as lower installation costs and costs to the consumer.

Although many lessons learned from EV battery development may be applied to the BTMS program, the requirements for BTMS systems are unique—carrying their own calendar-life, cycle-life, and cost challenges. For example, EV energy-storage systems need to meet very rigorous energy-density and volume requirements to meet consumer transportation needs. Despite that, current stationary storage systems use batteries designed for EVs due to high volumes that drive down costs. This creates another market demand for EV batteries, further straining the EV battery supply chain and critical-material demand.

By considering BTMS electrochemical solutions optimized for these applications with less focus on energy density in mass and volume, the potential for novel battery solutions is very appealing. Furthermore, the balance of plant (BOP) cost for a BTMS battery system—or, the cost of everything minus the battery cells—is thought to be upwards of 60% of the total energy-storage system cost. In contrast, the BOP costs of EVs make up roughly 30% of the total battery cost. Therefore, to realize desired cost targets, BTMS will also need to focus on reducing BOP cost through system optimization.

Design parameters are needed to optimize the BTMS system for performance, reliability, resilience, safety, and cost.

The objectives of the project are to:

- Produce BTM battery solutions that can be deployed at scale and meet the functional requirement of high-power EV charging.
- Use a total-systems approach for battery storage to develop and identify the specific functional requirements for BTMS battery solutions that will provide novel battery systems in the 1–10-MWh range at \$100/kWh installed cost—and that are able to cycle twice per day, discharging for at least 4 hours, with a lifetime of roughly 20 years or at least 8,000 cycles.

Approach

A cohesive multidisciplinary research effort—involving the National Renewable Energy Laboratory (NREL), Idaho National Laboratory (INL), Sandia National Laboratories (SNL), and Argonne National Laboratory (ANL)—will create a cost-effective, critical-materials-free solution to BTMS by employing a whole-systems approach. The focus of this initiative is to develop innovative battery energy-storage technologies with abundant materials applicable to PV energy generation, building energy-storage systems, EVs, and high-power charging systems. Solutions in the 1–10-MWh range will enable optimal integration of PV generation from a DC-DC connection, increase energy efficiency of buildings, eliminate potential grid impacts of high-power EV charging systems, and lower installation costs and costs to the consumer.

Many lessons learned from EV battery development may be applied to the BTMS program, but the requirements for BTMS systems are unique—carrying their own calendar-life, cycle-life, and cost challenges. For example, EV energy-storage systems need to meet very rigorous energy-density and volume requirements to meet consumer transportation needs. Despite that, current stationary storage systems use batteries designed for EVs due to high volumes that drive down the costs. This creates another market demand for EV batteries, further straining the EV battery supply chain and critical-material demand.

By considering BTMS electrochemical solutions optimized for these applications with less focus on energy density in mass and volume, the potential for novel battery solutions is very appealing. Furthermore, the BOP cost for a BTMS battery system, or the cost of everything minus the battery cells, is thought to be upwards of 60% of the total energy-storage system cost. In contrast, the BOP costs for EVs make up roughly 30% of the total battery cost. Therefore, BTMS will also need to focus on reducing BOP cost through system optimization to realize desired cost targets.

Integration of battery storage with PV generation, energy-efficient buildings, charging stations, and the electric grid will enable new and innovative control strategies. Design parameters are needed to optimize the BTMS system for performance, reliability, resilience, safety, and cost.

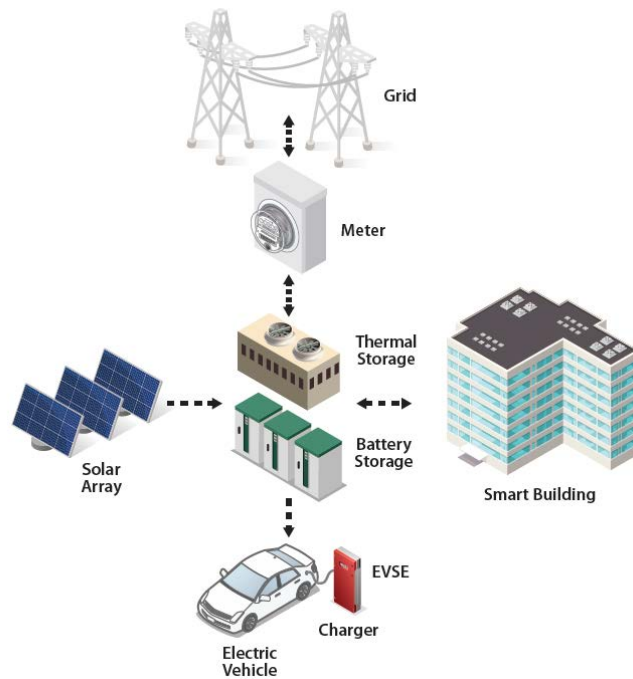


Figure 1. Overview of BTMS relevance.

Quarter 3 Milestone:

Due to the disruptions of the past quarter, all Q3 milestones have been delayed into Q4.

BTMS Analysis: Financial Metrics

National Renewable Energy Laboratory (NREL)

Margaret Mann, Madeline Gilleran, Chad Hunter, Darice Guittet, Matt Mitchell, Eric Bonnema, Jason Woods, Monisha Shah, Karl Heine

Summary

This Q3 Milestone report discusses the various financial metrics computed in the EnStore program and the preliminary methodology used to obtain these metrics. In determining and computing appropriate financial metrics, the “Manual for the Economic Evaluation of Energy Efficiency and Renewable Energy Technologies” was referenced and the existing System Advisor Model (SAM) cash-flow calculator was used, such that financial metrics are consistent with prior NREL and EERE research and tools (Short et al., 1995; Blair et al., 2018). Because a summary of range and probability distributions of EV electric load profiles was completed and reported on in the Q2 Milestone report, no further information will be provided in this report; but any questions regarding these results are welcome.

Background

The BTMS Analysis project is funded by the Buildings Technologies Office (BTO), Vehicle Technologies Office (VTO), and the Solar Energy Technologies Office (SETO) within the Department of Energy’s (DOE’s) Office of Energy Efficiency and Renewable Energy (EERE). The mission of EERE is to create and sustain American leadership in the transition to a global clean-energy economy. Its vision is a strong and prosperous America powered by clean, affordable, and secure energy. Increasing adoption of electric vehicles (EV), solar photovoltaic (PV) electricity generation, battery and thermal storage, and energy-efficient building technologies is expected to have a significant impact on energy use and domestic manufacturing. Although each of these technologies can make contributions to the U.S. economy, integrating them in ways that optimize cost and energy flows for varying energy demand and climate conditions across the country can lead to multiple positive impacts.

BTMS research is targeted at developing innovative energy storage technology specifically optimized for stationary applications that will enable fast charging of EVs, allow for enhanced grid-interactive energy-efficient buildings coupled with PV resources, all while minimizing grid impacts.

EV adoption is expected to grow significantly over the coming years, and it could have a significant, and potentially negative, effect on grid infrastructure due to large and irregular electricity demands. This is further complicated by the growth of variable-generation renewable energy technologies such as PV. In response to these changes, utilities are evaluating multiple options for managing dynamic loads, including time-of-use pricing and demand charges. Buildings and EV charging stations can leverage energy storage, including battery and thermal energy storage, coupled with on-site generation to stabilize the grid, manage energy costs, and provide resiliency and reliability for EV charging and building energy loads.

The key question in this project is the following: What are the optimal system designs and energy flows for thermal and electrochemical energy storage systems at sites with on-site PV generation and EV charging, and how do solutions vary with climate, building type, and utility rate structure?

Figure 1 is a high-level schematic depicting the various behind-the-meter systems, including stationary battery, solar PV, electric-vehicle supply equipment (EVSE), and thermal energy storage (TES).

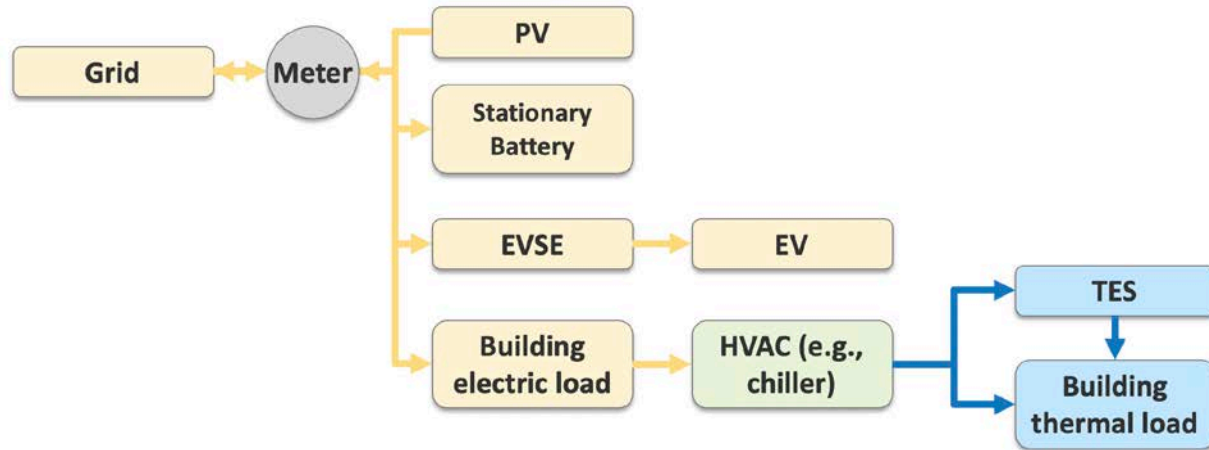


Figure 1. Schematic depicting the default combination of technologies for BTMS analysis.

The BTMS Analysis team is developing a multi-tool simulation platform called EnStore, short for Energy Storage. This platform will be able to capture performance characteristics and interactions between disparate technologies with high fidelity. *In researching existing tools used in this space, the team concluded that no one existing tool could complete the multisystem, detailed analysis required for this project—but rather, a combination of several existing tools would be necessary.* This project will leverage the following tools:

- REopt™ energy-system optimization tool (Cutler et al., 2017)
- System Advisor Model (SAM) (Blair et al., 2018)
- EV-EnSite and Electric Vehicle Infrastructure Projection Tool (EVI-Pro) (Ucer, Wood et al., 2018)
- EnergyPlus™ building simulation engine (DOE, 2019a)
- OpenStudio® suite of supporting building simulation applications (DOE, 2019b)
- Utility Rate Database (URDB) (DOE, 2019c)
- The DOE Prototype building energy models (DOE, 2019d).

Financial Metrics Captured in EnStore

This section discusses the various financial metrics captured in EnStore. Initial focus for the analysis and methodology is around a single ownership model, where one entity owns the building, the EV charging station, and any BTMS equipment, including the stationary battery, solar PV, and TES. Therefore, all the BTMS costs and benefits accrue to a single owner. This may not be representative of the market today, because places such as Walmart may have EV stations owned and operated by Electrify America and that are separately metered. However, this model still provides a starting point for BTMS system comparisons. We will continue to explore other ownership models, try to identify which are the most prevalent, and determine the appropriate financial metrics for these disaggregated ownership models in the future.

Three financial metrics will be used to understand the economic impact of BTMS to the system owner including: net present cost (NPC), levelized cost of charging (LCOC), and levelized cost of electricity (LCOE).

- **NPC** is defined as the total present cost of the system to the system owner. Note that net present value and the net present cost differ only in sign.
- **LCOC** is the minimum required selling price that the owner of the system must charge EV owners in order to “break even” after paying for the capital and operating expenses with a specified rate of return. At a high level, LCOC is computed by identifying all the system costs beyond the building electricity costs, and then determining what EV owners must pay (\$/kWh) to achieve a net present

value (NPV) equal to zero. It is important to note that the LCOC is not the market price for EV charging, because the market may be willing to pay more or less than this amount; the true market value for EV charging is unknown in this analysis.

- **LCOE** is analogous to LCOC, but instead, it is computed from the building’s perspective (e.g., all marginal systems costs and benefits accrue to the building).

In this analysis, we compare each of the financial metrics of a baseline (with a “seed” building with EV charging stations but no BTMS system [battery, PV, TES]) with the financial metrics of the full BTMS system, including the building and EV charging station. The baseline scenario provides the benchmark for the system owner to use when determining if the BTMS system is economically attractive. In the baseline scenario, it is important to note that the EV station and the building being under the same meter is implied and exist before any BTMS equipment is installed.

Net Present Cost

NPC is defined as the sum of all the discounted costs of the entire system over the lifetime of the project. NPC can be computed for a baseline system (building and EVSE infrastructure) as well as the BTMS system (building, EVSE infrastructure, and the new battery, PV, and TES assets). By computing the NPC for both systems, the metric can be used to help answer a key research question:

- *Should the system owner install the BTMS equipment or not?*

NPC is the most straightforward to calculate of the three financial metrics discussed above because all the costs and benefits of the BTMS system are accrued to a single owner.

Understanding that the NPC for the multi-asset BTMS system will have higher upfront capital costs than that of the baseline system (with no initial capital costs), the future lower operational costs from saving money on the annual electricity bill must at some point allow the system owner to “break even” and cover the initial investment costs. If the BTMS system is worth the investment, then the annual electricity bill must be low enough such that the NPC of the BTMS system is lower than that of the baseline system.

Mathematically, NPC includes capital costs, fixed and variable operational costs, and the monthly utility bill, which is another type of operational cost. Costs that are incurred over time are discounted back to present values using a discount rate representing the risk-adjusted, time-value of money.

$$NPC = \text{Discounted CapEx} + \text{Discounted Fixed OpEx} + \text{Discounted Variable OpEx} + \text{Discounted Monthly Utility Bill.}$$

CapEx, or capital expenditures, for the BTMS case include all upfront installed costs, including the battery, solar PV, thermal energy storage, EVSE, power electronics, interconnection, and BOP. CapEx for the baseline system (with building + EV charging station only) include only that of the EVSE, interconnection cost, and related power electronics components.

OpEx, or operational expenditures, for the BTMS case could include the energy costs, maintenance labor, and maintenance supplies for the battery, solar PV, TES, or EVSE. The annual electricity cost is broken out in the formula above for convenience with later calculations.

NPC can be written mathematically as:

$$NPC = \sum_i C_i + \sum_n \left[\frac{\sum_i (F_{i,n} + V_{i,n}) + \sum_m M_m}{(1 + r)^n} \right]$$

where

- $i = \text{asset } i$
- $n = \text{period (e.g., year)}$
- $m = \text{subperiod (e.g., month)}$
- $C_i = \text{capital cost of asset } i$
- $F_{i,n} = \text{fixed cost of asset } i \text{ in period } n$
- $V_{i,n} = \text{variable cost of asset } i \text{ in period } n$
- $M_m = \text{subperiod (e.g., month) utility bill for subperiod } m$
- $r = \text{discount rate per period.}$

Levelized Cost of Charging (LCOC)

LCOC is defined as the minimum required selling price of the electricity sold to the EV owners to pay back all costs associated with the project at the specified rate of return. LCOC can be computed for the baseline scenario (building and EV charging station only) and the BTMS scenario (building, EV charging station, battery, PV, and TES) to help answer the research question:

- *If BTMS equipment were installed, what would be the relative impact to the EV owner?*

Example output would be similar to the following:

- $LCOC_{baseline} = \$0.15/kWh$
- $LCOC_{BTMS} = \$0.10/kWh,$

which would be able to inform the system owner that the project is both economically attractive (because $LCOC_{BTMS}$ is less than $LCOC_{baseline}$) and lowers the required EV electricity selling price to break-even by 33%.

To compute LCOC and have it provide information beyond the NPC metric, the relative costs of the EV charging station and building must be disaggregated and allocated to each subsystem (building or EV owners). For example, in the baseline scenario (building and EV charging station only), the LCOC must be computed to represent the effective cost of electricity sold to the EV owners while the building pays its “fair share” of the total system utility bill. A combined building and EV charging-station utility bill may not simply be the sum of two separate utility bills (due to non-linear demand charges), so the following assumptions are made:

1. The building will pay a utility bill equal to that if the EV charging station did not exist, and
2. The EV owners will pay for all marginal costs associated with installing and using the EV charging stations (marginal demand charges, marginal energy consumption, marginal asset costs [e.g., EVSE, controls]).

The assumption that the EV owners pay for all marginal costs is justified because vehicle owners have 1) a more inelastic demand for energy prices and 2) a higher willingness-to-pay for electricity than a building owner would. With those two assumptions, the LCOC for a baseline system can be calculated by removing the building electricity costs associated with only the building and normalizing by the total energy consumption of the EVs. Mathematically:

$$LCOC_{baseline} = \left(\frac{C'_{EVSE+building} - C'_{baseline \text{ building only}}}{E'_{BEV}} \right)$$

where

- $C'_i = \text{vector of discounted cash flows (costs) for system } i$
- $E'_i = \text{vector of discounted energy flows going to item } i$
- $BEV = \text{battery electric vehicle.}$

Specifically, $C'_{EVSE+building}$ represents the vector of cash flows for the baseline system (building with the EV charging station), whereas $C'_{baseline\ building\ only}$ denotes the cash flows for the annual electricity bill of the building. By removing the building cost from the baseline system, only marginal costs related to the addition of the EV charging infrastructure are left, which can be normalized by the battery EV charging to obtain an LCOC.

Expanding the above equation into the summation over the periods yields:

$$LCOC_{baseline} = \left(\frac{\sum_i C_i + \sum_n \left[\frac{\sum_i (F_{i,n} + V_{i,n}) + \sum_m M_m}{(1+r)^n} \right] - \left(C_b + \sum_n \left[\frac{F_{b,n} + V_{b,n} + \sum_m M_{b,m}}{(1+r)^n} \right] \right)}{\sum_n \left[\frac{E_n}{(1+r)^n} \right]} \right)$$

or, more succinctly:

$$LCOC_{baseline} = \left(\frac{\sum_i [C_i] - C_b + \sum_n \left[\frac{\sum_i (F_{i,n} + V_{i,n}) - F_{b,n} - V_{b,n} + \sum_m (M_m - M_{b,m})}{(1+r)^n} \right]}{\sum_n \left[\frac{E_n}{(1+r)^n} \right]} \right)$$

where

- $i = asset\ i$
- $n = period\ (e.g.,\ year)$
- $b = building\ (subscript)$
- $m = subperiod\ (e.g.,\ month)$
- $C_i = capital\ cost\ of\ asset\ i$
- $F_{i,n} = fixed\ cost\ of\ asset\ i\ in\ period\ n$
- $V_{i,n} = variable\ cost\ of\ asset\ i\ in\ period\ n$
- $M_m = subperiod\ (e.g.,\ month)\ utility\ bill\ for\ subperiod\ m$
- $r = discount\ rate\ per\ period$
- $E_n = BEV\ charging\ energy\ (e.g.,\ kWh)\ in\ period\ n.$

As seen in this equation, the removal of the baseline-building-only costs can be any capital, fixed, or variable costs associated with the building. However, it is likely that only a monthly utility bill of the baseline building will need to be removed to calculate the LCOC metric.

The LCOC of the BTMS system can be computed in an analogous way but replacing the baseline system costs with the BTMS system costs. Mathematically, this can be expressed as:

$$LCOC_{BTMS} = \left(\frac{C'_{EVSE+building+BTMS} - C'_{baseline\ building\ only}}{E'_{BEV}} \right)$$

By computing the LCOC metric in this way for both the baseline scenario and the BTMS scenario, the metric can be used to inform both the system owner on the economic attractiveness of the project while also providing information on the relative impact to the EV owners.

Also, it should be noted that that impact of taxes, carry-forward tax losses, and incentives are not explicitly shown in these equations for clarity but will be accounted for in the actual computation within EnStore.

Levelized Cost of Electricity (LCOE)

LCOE is defined as the minimum required selling price of the electricity sold to the building owner to pay back all costs associated with the project at the specified rate of return. It answers the research question, “If BTMS equipment were installed, what are the financial benefits of the investment to the building owner?”

Mathematically, this is very similar to the LCOC calculation except it assumes that all benefits of the BTMS system go to the building owner as opposed to the EV owner. Thus, the calculations for LCOE are similar to those of LCOC, but levelization is by energy usage of the building as opposed to energy usage of the EVSE.

All marginal costs of adding the EV station accrue to the EV owners, so the LCOE for the building is trivial and is effectively the levelized utility rate for the building:

$$LCOE_{baseline} = \left(\frac{C'_{baseline\ building\ only}}{E'_{building}} \right)$$

where

C'_i = vector of discounted cash flows (costs) for system i

E'_i = vector of discounted energy flows going to item i .

The LCOE of the BTMS system can be computed in an analogous way but replacing the baseline system costs with the BTMS system costs. Mathematically, this can be expressed as:

$$LCOE_{BTMS} = \left(\frac{C'_{EVSE+building+BTMS} - [C'_{EVSE+building} - C'_{baseline\ building\ only}]}{E'_{building}} \right)$$

Thus, by defining the LCOE of the building in this way, it can be used to determine if the BTMS system is economically attractive ($LCOE_{BTMS}$ is less than $LCOE_{baseline}$) and the relative impact to the building owner assuming all benefits are accrued to the building (e.g., by what percentage was $LCOE$ reduced due to the BTMS investment).

Using consistent accounting allows us to compute both LCOC and LCOE. These metrics provide additional information beyond the NPC metric and help answer additional research questions, such as, “What is the relative impact to the individual EV owners or building rate payer?”

Single Owner vs. Multiple Owner Business Models

Multiple ownership models will be evaluated in detail in FY21 to better understand how asset ownership structure impacts the decision about whether or not to invest in this BTMS equipment. This will involve developing a better understanding of the common business models seen today or could be used in the future, identifying how interactions and agreements between owners will be handled, and determining the relative cost impacts within and across owner boundaries.

Where Financial Metrics are Computed in EnStore

The financial metrics are crucial for the EnStore program because the cost analysis helps determine how various details of the BTMS system balance and interact, and they are a main way to determine the economic value and attractiveness of the BTMS system. This section describes where financial metrics are computed in EnStore, detailing how the program finds the BTMS configuration that leads to the greatest financial savings for the system owner. A graphic depicting the various stages of EnStore can be seen in Figure 2.

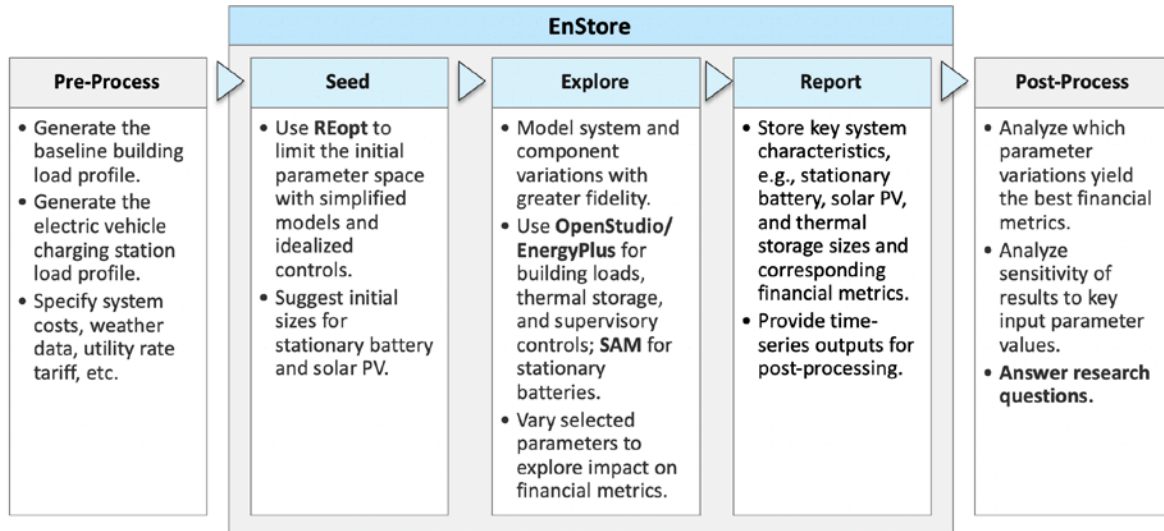


Figure 2. Schematic depicting EnStore workflow.

In the Seed Stage of the EnStore program, REopt will first calculate preliminary optimal sizes for the stationary battery system and PV system, finding those that maximize the net present value (NPV) of the system. Next, the Exploration Stage of the EnStore program is used to consider higher-fidelity, physics-based models of load, generation, and storage systems to increase the accuracy of electrical power and heat-transfer calculations. At this stage, EnStore will use OpenStudio, EnergyPlus, and SAM to examine how inclusion of more detailed component performance characteristics and system interactions can affect design optimization results. For each EnergyPlus simulation in the Exploration Stage, permutations of the solar PV size, TES size, and stationary battery size will occur. They will differ from those of REopt. Perhaps there will be 10 permutations of solar, TES, and stationary battery sizes each, which means there will be $10 \times 10 \times 10$, or 1000, total simulations occurring for one single REopt run, to determine the optimal configuration of these systems.

For each of the hypothetical 1000 runs mentioned above, the run with the lowest cost computed in financial calculations will be that which has the “optimal configuration.” As mentioned previously, the cost metrics calculated will either be NPC, LCOC, or LCOE, depending on the scenario of interest. Because the energy usage of the EV charging station and the seed building is fixed beforehand, the configuration with the lowest NPC will match that with the lowest LCOC and LCOE. Therefore, the run with the minimum associated NPC, LCOC, and LCOE for a given utility rate, location, building type, unit costs, and more will be stored, and its respective BTMS configuration of sizes will be reported.

Methodology for Computing Financials in EnStore

We will be leveraging established SAM modules for the financial analysis. Specifically, we will be using the PySAM UtilityRate5 and CashLoan modules to compute financial metrics. The UtilityRate5 module computes the annual electricity bill using a regionally and temporally resolved utility rate. The utility bill is included in cash-flow calculations as an operational expense that is incurred over each year of the project. The CashLoan module will be used to compute NPC and LCOC/LCOE, considering the discount rate, state and federal tax incentives, investment or production tax credits, and more. Documentation for the UtilityRate5 module can be found [here](#); documentation for the CashLoan module can be found [here](#).

The UtilityRate5 module will receive necessary “gen” and “load” input vectors, or generation and load vectors, from the EnergyPlus timeseries outputs. The load vector is equivalent to the load of the building + EVSE after BTMS has lowered its demand and is the net electricity bought from the grid, or “grid to system.” In

EnergyPlus, this is denoted as ElectricityPurchased:Facility [J](TimeStep). The gen vector is equivalent to the net electricity sold to the grid, or “system to grid.” In EnergyPlus, this is denoted as ElectricitySurplusSold:Facility [J] (TimeStep). These net loads and the utility rate information are sufficient to compute the annual electricity bill, which is one of the inputs to the CashLoan module.

The CashLoan module takes in all installed costs and annual O&M costs, including the annual electricity bill, and uses this alongside information such as the discount rate, federal and state tax rate, and inflation rate to compute the LCOC, LCOE, and NPC.

References

- Blair, N., N. DiOrio, J. Freeman, P. Gilman, S. Janzou, T. Neises, M. Wagner. 2018. System Advisor Model (SAM) General Description (Version 2017.9.5). Golden, CO: National Renewable Energy Laboratory (NREL). NREL/TP-6A20-70414. <https://www.nrel.gov/docs/fy18osti/70414.pdf>.
- Cutler, D., D. Olis, E. Elgqvist, X. Li, N. Laws, N. DiOrio, A. Walker, K. Anderson. 2017. REopt: A Platform for Energy System Integration and Optimization. Golden, CO: National Renewable Energy Laboratory (NREL). NREL Technical Report No. NREL/TP-7A40-70022. <https://www.nrel.gov/docs/fy17osti/70022.pdf>.
- Dey, S., Y. Shi, K. Smith, A.M. Colclasure, X. Li. 2020. “From Battery Cell to Electrodes: Real-Time Estimation of Charge and Health of Individual Battery Electrodes.” IEEE Transactions on Industrial Electronics 67, no. 3: 2167–75. <https://doi.org/10.1109/TIE.2019.2907514>.
- DOE (U.S. Department of Energy). 2019a. “EnergyPlus.” <https://www.energyplus.net>.
- DOE (U.S. Department of Energy). 2019b. “OpenStudio.” <https://www.openstudio.net>.
- DOE (U.S. Department of Energy). 2019c. “Utility Rate Database.” https://openei.org/wiki/Utility_Rate_Database.
- DOE (U.S. Department of Energy). 2019d. “Commercial Prototype Building Models.” https://www.energycodes.gov/development/commercial/prototype_models.
- Short, W., D.J. Packey, T. Holt. 1995. “Manual for the Economic Evaluation of Energy Efficiency and Renewable Energy Technologies.” NREL Technical Report. <https://www.nrel.gov/docs/legosti/old/5173.pdf>.
- Ucer, E., M. Kisacikoglu, F. Erden, A. Meintz, C. Rames. 2018. “Development of a DC Fast Charging Station Model for use with EV Infrastructure Projection Tool.” 2018 IEEE Transportation Electrification Conference and Expo (ITEC): 904-909. <https://doi.org/10.1109/ITEC.2018.8450158>.
- Wood, E., C. Rames, M. Muratori. 2018. “New EVSE Analytical Tools/Models: Electric Vehicle Infrastructure Projection Tool (EVI-Pro).” Golden, CO: National Renewable Energy Laboratory (NREL). NREL Presentation No. NREL/PR-5400-70831. <https://www.nrel.gov/docs/fy18osti/70831.pdf>.

BTMS Power Electronics for Behind-the-Meter Storage

National Renewable Energy Laboratory
Ahmed Mohamed, Ram Kotecha, Andrew Meintz

Background

The power electronics effort for BTMS has been tasked with evaluating methods to reduce the balance-of-plant (BOP) cost associated balance-of-plant components for a stationary battery system. The technology target for the entire BTMS system ranges from \$295/kWh to \$235/kWh for a C/1 or C/4 charging-station target. The BOP, including the power conversion, is roughly two-thirds of the system cost. From a power perspective, the BOP equates to between \$0.195/W and \$0.540/W between the two station designs (C/4 and C/1). In the FY19 analysis of current-state stationary energy storage systems considering at least a 1-MW system with a 13.8-kV connection, the BOP costs ranged from \$0.40 to \$1.01/W. An investigation of the various power conversion topologies (ac-coupled, dc-coupled, and multiple bus dc-coupled) will be investigated to determine strategies for the entire site to optimize the design of the BOP. The task objectives for investigation of the primary power conversion optimization are as follows:

- Explore different configurations for integrating ~2-MW dc fast-charging (DCFC) loads, ~2-MW photovoltaic (PV) generation, and ~2-MW energy storage system (ESS) with the power grid:
 - Conventional common ac bus configuration.
 - New common dc bus configuration.
 - Modular-based multiple dc bus.
- Estimates efficiency vs. load curve for the power electronic conversion stages for:
 - DC fast chargers (350 kW ports).
 - PV generation.
 - Grid energy storage system.
 - Grid interface (e.g., transformer, and ac/dc converter).
- Integrate the conversion efficiency data with EnStore platform for system cost analysis.

Results

The team has defined the possible configuration for a site integrated with ~2-MW DCFC loads, ~2-MW PV generation, and ~2-MW ESS with the power grid. Three different configurations are considered:

- A. Conventional common ac bus configuration:

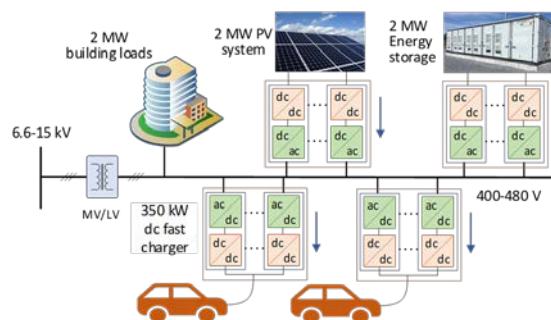


Figure 1. Conventional common ac bus integration.

- B. Common dc bus configuration:

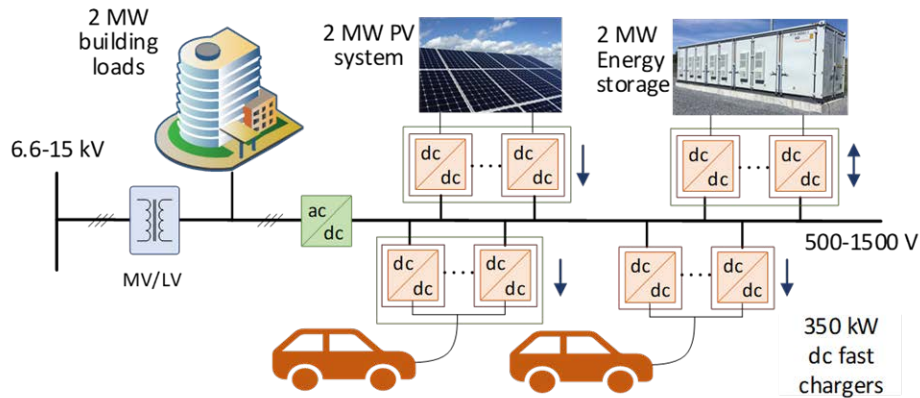


Figure 2. Common dc bus microgrid integration.

C. Modular-based multiple dc bus configuration

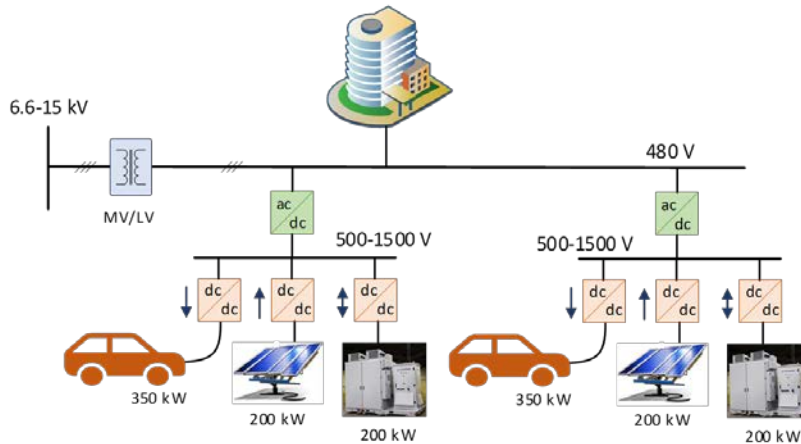


Figure 3. Modular-based multiple dc bus microgrid integration.

Conventional common ac bus configuration

- In this quarterly report, NREL’s Power Electronics (PE) team focused on the conventional common ac bus configuration (Figure 1) as a base case that represents the current situation with the commercially available devices, including PV inverter, DCFC, and ESS converter. In this configuration, all generations and loads are coupled to the grid through a common LV (480 V) ac bus. A MV/LV transformer is used to bring the voltage down. PV, ESS and DCFC are connected to the ac bus through two conversion stages ac/dc and dc/dc. Modular concept is considered to size the 2-MW system level. For evaluating this configuration, commercial components available at the Energy Systems Integration Facility (ESIF, at NREL) are considered.
- Starting with the PV system, the EnStore platform incorporated the System Advisor Model (SAM) to model the PV system performance. SAM includes a database for several commercially available PV inverters and uses the Sandia inverter model to predict the PV system performance, as indicated in Fig. 4 [1–2].

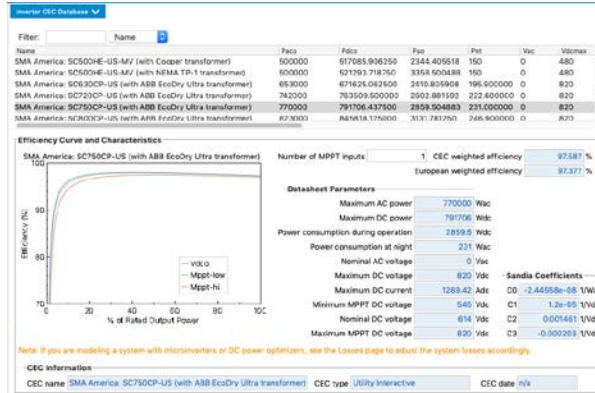


Figure 4. Description of efficiency data of PV inverter in the System Advisor Model (SAM).

- The Sandia PV inverter power model is an empirically based performance model of inverter performance that uses parameters from a database of commercially available inverters maintained by the California Energy Commission (CEC). It estimates the ac output power as function of dc input power and dc input voltage [3]. This model is applicable for PV inverter only, in which the power moves from the dc to ac side. The model is not appropriate for EV charging application, in which the power flows from ac to dc. In addition, it is not applicable for the bidirectional operation associated with the ESS. Therefore, it is necessary to develop a new model that is able to predict the performance of DCFCs and ESSs.

NREL Generic Converter Power Model

- This model is an empirically based performance-generic model for different converters. It estimates the output power and efficiency in terms of input power and dc bus voltage. The model uses parameters from the datasheet of commercially available converters as well as actual tests. The model is generic and applicable for different converters for different applications, including PV inverter, DCFC, and bidirectional converter. The model is described in Figure 5 and stated mathematically in (1)–(3).

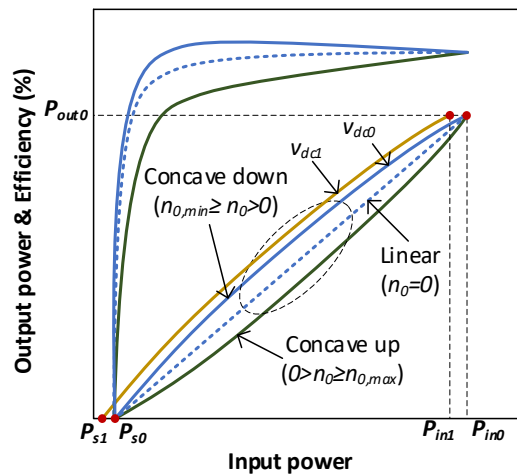


Figure 5. Converter power and efficiency model.

$$P_{out} = \left(\frac{P_{out0}}{P_{in0} - P_{s0}} \right) (P_{in} - P_{s0}) - \frac{n_0(P_{in0} - P_{in})(P_{in} - P_{s0})}{P_{in0}} \quad (1)$$

where:

P_{out} : output power from the converter, (W)

P_{in} : input power to the converter, (W)

P_{out0} : maximum output power “rating” for converter at the standard test condition, assumed to be an upper limit value, (W)

P_{in0} : input power at which P_{out0} is achieved at the standard test condition, (W)

P_{s0} : standby power at which the conversion process starts at standard test condition, (W)

n_0 : nonlinearity factor defining the curvature of the relationship between input and output power at the standard test condition.

- The impact of variation of dc bus voltage (whether on the input or the output side) is considered using (2).

$$\begin{aligned} P_{ac1} &= P_{ac0}[1 + C_1(V_{dc1} - V_{dco})] \\ P_{s1} &= P_{s0}[1 + C_2(V_{dc1} - V_{dco})] \\ n_1 &= n_0[1 + C_3(V_{dc1} - V_{dco})] \end{aligned} \quad (2)$$

C_1 : empirical coefficient allowing P_{in0} to vary linearly with dc-voltage input, default value is zero, (1/V)

C_2 : empirical coefficient allowing P_{s0} to vary linearly with dc-voltage input, default value is zero, (1/V)

C_3 : empirical coefficient allowing n_0 to vary linearly with dc-voltage input, default value is zero.

- Nonlinearity factor is an empirical parameter that defines the nonlinearity in the relationship between input and output power, as described in (3). For the concave-up and linear models, the maximum efficiency occurs at the rated power. For the concave-down model, the maximum efficiency occurs before the rated power. Impact of the nonlinearity factor on the power and efficiency curve is indicated in Fig. 6.

$$n_0 = \begin{cases} n_0 = 0 & \text{Linear} \\ n_{0,min} \geq n_0 > 0 & \text{Concave down} \\ 0 > n_0 \geq n_{0,max} & \text{Concave up} \end{cases} \quad (3)$$

$n_{0,max}$ is very close to 1 (~0.9)

$n_{0,min}$ varies based on the rated and standby powers. It is very close to -0.1

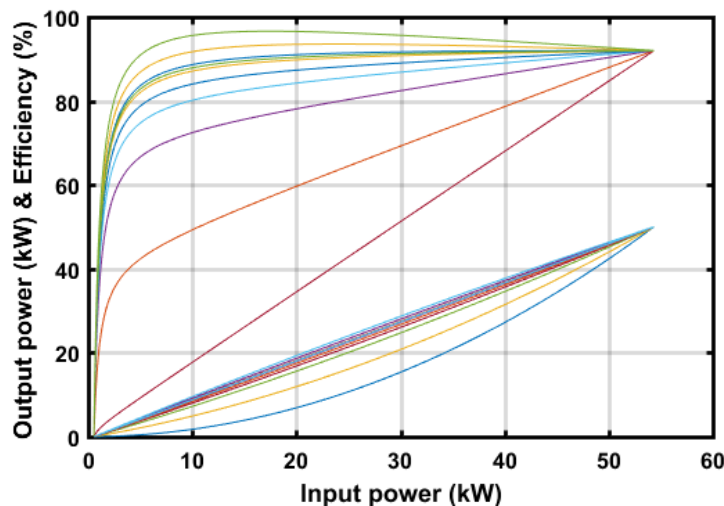


Figure 6. Impact of nonlinearity factor on the power model.

Applying the NREL Generic Model for DCFC

- The NREL PE team has used the model to predict the performance of DCFCs. A list of DCFC equipment available at ESIF is presented in Table 1. It shows a variety of commercial DCFCs with different power levels and manufactures. These devices will be tested, and the associated model parameters will be extracted.

Table-1: List of commercial DCFCs planned for testing at NREL

Model	P_{in0} (kW)	P_{out0} (kW)	V_{ac} (V)	P_{s0} (W)	V_{dc0} (V)	Efficiency	
						Maximum	Minimum
ABB-Terra-HPC (1x175)	175	160	480/277	≤ 80	150-920	95.51	94%@20% load
ABB-Terra-HP (2x175)	350	320	480/277	≤ 80	150-920	95.51	94%@20% load
BTC-HP (2x50)	86.10	80	480	-	50-950	93.518	92%
BTC-350-HP (8x50)	376.7	350	480	-	50-950	93.518	92%
Tritium-50-HP	55	50	480/277	-	300-600	93.518	92%
ABB Terra 50	49.7	45.9	480	99	397	92.8	79.8

- As an example, the NREL PE team leveraged the test data for the ABB-Terra-50 published by Idaho National Laboratory (INL) [4]. The measurements are shown in Fig. 6, which shows $P_{out0} = 45.9$ kW, $P_{in0} = 49.7$ kW, $\eta_0 = 92.3\%$, $P_{s0} = 99$ W, and $\eta_{max} = 92.8\%$. These data are digitalized and used to estimate the model parameters associated with the DCFC, as indicated in Figs. 7 and 8. Only the orange part in Fig. 8 is considered for estimating the model parameters to avoid the misleading points.

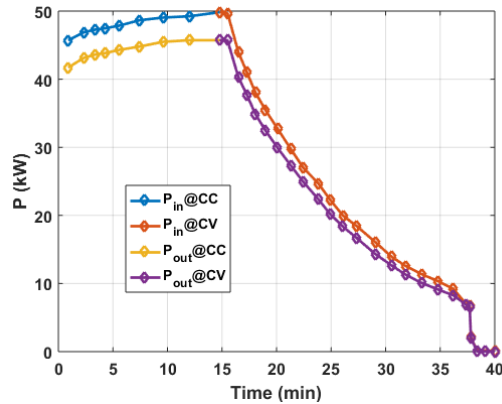


Figure 7. Measured input and output power profile with time of ABB-Terra-50 published by INL [4].

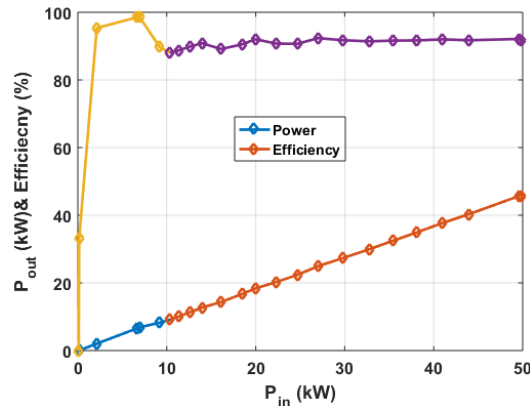


Figure 8. Output power and efficiency versus input power of ABB-Terra-50 published by INL [4].

- These measured data are fitted to the model to estimate the nonlinearity factors that match these measurements. A comparison between the model output and the measurements is indicated in Fig. 9, which shows very good correlation at a nonlinearity factor of 0.0121.

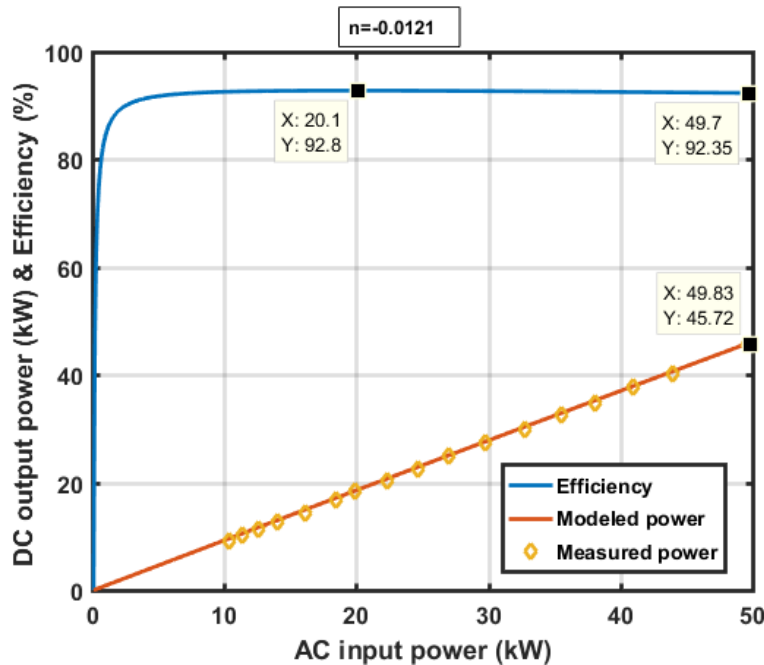


Figure 9. Measured and modeled power and efficiency curve for ABB-Terra-50.

- The parameters provided in the manufacturer datasheet (Table 1), along with assumptions made based on the current literature, will be considered to estimate the parameters for the other DCFCs’ model.

Conclusions

The team has begun an integrated discussion with the cost analysis team on investigating the various power conversion topologies (ac-coupled, dc-coupled, and multiple bus dc-coupled). The team developed a generic power model that is applicable for dc/ac conversion (e.g., PV), ac/dc conversion (e.g., DCFC), and bidirectional conversion (e.g., ESS). The model is applied for the ABB-Terra-50 DCFC and shows very good correlation with the measurements. This model is provided to the cost analysis team, along with a database for the commercially available DCFCs at NREL developed with the associated parameters to be integrated with the EnStore platform. The estimation approach outlined above will support “datasheet” conversion efforts, although the team intends to leverage other activities to refine these models for actual equipment available in the ESIF. The task objectives for investigating the primary power conversion are expected to support a broader understanding of which scenarios (based on, e.g., energy throughput, onsite equipment) will benefit from these new approaches to identify operational benefits.

References

1. Gilman, P.; Dobos, A.; DiOrio, N.; Freeman, J.; Janzou, S.; Ryberg, D. (2018) SAM Photovoltaic Model Technical Reference Update. 93 pp.; NREL/TP-6A20-67399. ([PDF 1.8 MB](#)).
2. Gilman, P. (2015). SAM Photovoltaic Model Technical Reference. National Renewable Energy Laboratory. 59 pp.; NREL/TP-6A20-64102. ([PDF 1.8 MB](#)).

3. King, D.L.; Boyson, W.E.; and Kratochvil, J.A. (2004). Photovoltaic Array Performance Model. 41 pp.; Sandia Report No. 2004-3535. ([PDF 1.8 MB](#)).
 4. <https://avt.inl.gov/sites/default/files/pdf/evse/ABBDCFCFactSheetJune2016.pdf>
-

BTMS Testing

Contributors: INL, Electric Applications Incorporated, SNL, NREL

Background

An ongoing task is the assessment of possible electrochemical energy storage chemistries that have the capability of meeting the BTMS targets. In the last quarter, we expanded our cell chemistries to include nickel-zinc and lead acid.

Lead Acid Testing

In the last quarter, we added Electric Applications Inc. (EAI) to the team to evaluate potential lead acid configurations. Current limitations on the energy density of lead batteries are clearly an issue in mobile applications. However, these limitations play a lesser part in stationary storage applications, and improvements in material utilization are clearly achievable. Currently, a typical lead battery operates at 35 Wh/kg. This is less than 20% of the theoretical energy density for lead of 190 Wh/kg, shown in Figure 1, thus leaving significant opportunity for improvement.

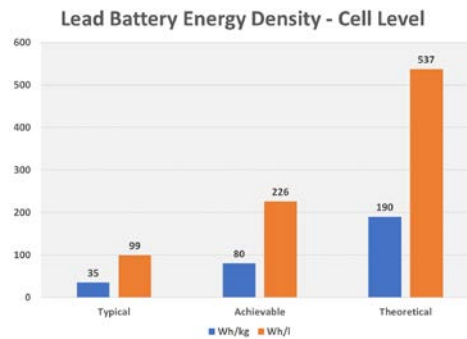


Figure 1. Energy density possibilities for lead acid batteries.

Other issues, most significantly cycle life in energy storage applications, are currently unknown relative to the capability of lead batteries to compete on a total cost of ownership (TCO) basis with lithium technology. To quantify the drivers of lead battery grid energy storage TCO, EAI has been charged with testing both conventional and emerging lead battery technologies in a simulated EV fast-charge demand-reduction application.

Cycle-Life Test Refinement and Testing

Idaho National Laboratory (INL) and EAI collaborated with the BTMS team to refine the test cycle presented last quarter, simulating the device-level power profile from the battery of a peak-shaving system supporting an extreme fast charger. A test cycle has been developed, shakedown tested on surrogate cells, and will be used to evaluate the cycle-life performance of various lead battery technologies at EAI, and other critical-material-free battery technologies at INL, Sandia National Laboratories (SNL), and NREL. These data are complemented by continuing benchmark testing of commercial cell technologies that was started at the onset of the BTMS project. The resulting data will be used by the BTMS project team as an input to an overarching analysis project focused on optimizing BTMS for several applications.

Results

Cycle-Life Test Shakedown and Refinement

Work among testing labs continued to evaluate the test protocol presented last quarter by applying it to surrogate cells, and then to use the results of that shakedown testing to refine the test cycle to simulating cases of grid power demand-reduction application for a high-power EV fast charger. Three cycles were preliminarily evaluated, each anticipating a different number of vehicles presenting themselves for charging and a different

timing of the vehicle arrivals. Battery sizing was based on how many vehicles would need to be supported for peak 10-minute, back-to-back (i.e., one immediately after the other) charges. Components of the preliminary cycles were discussed with the BTMS team and reduced to two cycles to be applied across all device types to be tested, such that the results can be compared across various technologies.

Two test cycles have been established for cycle-life testing. Both cycles accommodate 24 vehicles per day conducting fast charges at peak station power for 10 minutes each. The two test cycles evaluate the effect of the corner cases of arrival times of the vehicles at the charger. One cycle assumes that 12 vehicles arrive one immediately after another, such that the device's usable energy is discharged continuously over a two-hour period. There is then a 10-hour period where no vehicles arrive at the charger and the device can be fully recharged. This cycle is repeated to cycle the device's usable energy twice in a 24-hour day. This cycle is intended to represent a charger that operates with a morning rush and an evening rush, servicing 24 vehicles per day at peak power.

The other test cycle also services 24 vehicles per day. However, for this test cycle, the 10-minute charges at peak power are separated by periods of about 26 minutes, during which no vehicle charging occurs, and the device under test is partially recharged. In this cycle, all 24 vehicles to be serviced daily by the fast charger arrive one after another with this separation of 36 minutes (10 minutes of vehicle charging plus a 26-minute quiet period). After charging the 24 vehicles, the charger finishes its 24-hour day with a 10-hour period where no vehicles arrive at the charger. This cycle is intended to represent a charger that operates consistently and evenly throughout the daytime hours.

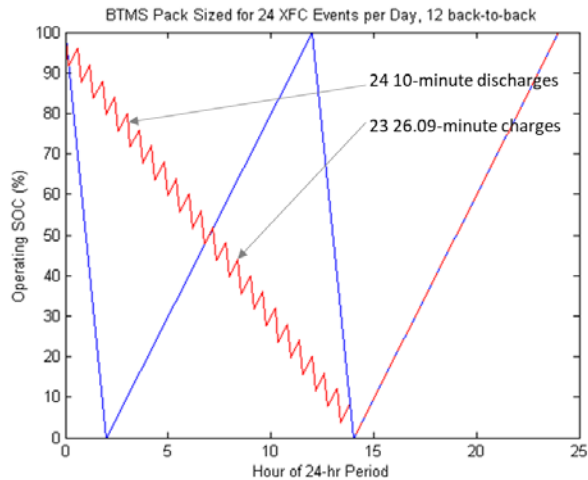


Figure 2. Charge-discharge protocol for BTMS.

The purpose of a demand-reduction energy storage system is to reduce the power demand on the electric grid from operation of the EV fast charger. With no demand reduction, the electric grid must supply the full peak vehicle charge power. If this vehicle charging power can be optimally buffered, the theoretical minimum electric grid power required to service 24 vehicles in a 24-hour period would be less than 20% of the peak fast-charger input power, supplied continuously, spread over the 24-hour day. Using battery energy storage to buffer vehicle-charging power, resulting from the two BTMS test cycles described above, results in operation of the energy storage battery as shown in Figure 3. The operating state of charge (SOC) in this figure represents the percent of the operating range of the battery—for example, from 100% battery SOC to 30% battery SOC, where 30% battery SOC is the minimum recommended battery discharge level and corresponds to 0% operating SOC. The blue line depicts the battery operation (as defined by the operating SOC) for the morning and afternoon rush test cycle. The red line depicts battery operation for the even distribution of vehicle charging during the daytime hours.

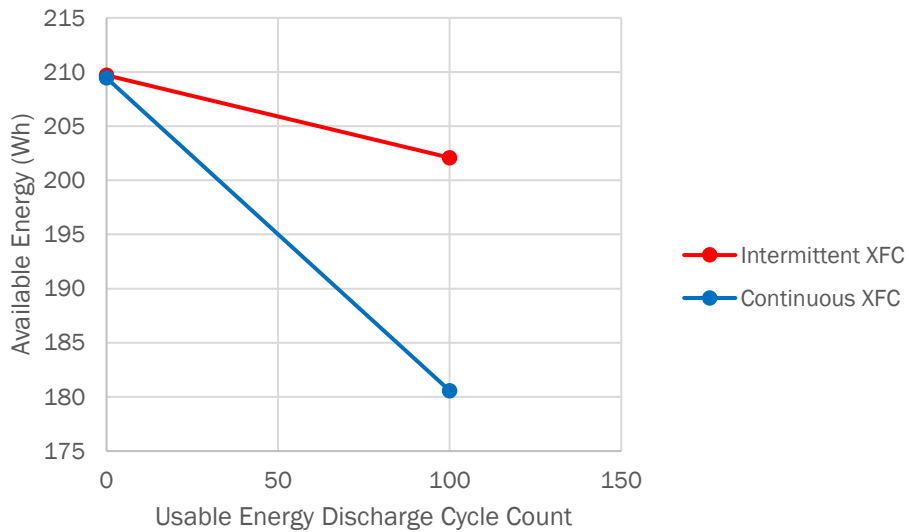


Figure 3. Differences in operating range of the battery in the two BTMS testing protocols.

The procedure to determine device-level power targets to support the two cycles was executed on a set of commercial NMC/Graphite cells. The cells were then cycled using both cycle profiles, although to acquire results faster, a 2-hour discharge period was combined with a 3-hour recharge period, resulting in 3 cycles of the cells’ usable energy every 25 hours. The discharge power was identical for the cells operating under both profiles, and the charging routine was also identical between the two cells, where a CP-CV charging strategy was used. After 100 cycles of the cells’ usable energy, a continuous constant power discharge test was performed—from the operating maximum voltage down to the minimum cutoff voltage for the cells.

The resulting difference in energy fade among the two cells shows that the two cycle profiles can result in different aging of the cells. The shakedown testing continues, although these preliminary results show it is important to use both profiles: despite cycling the same gross energy throughput per day, and exercising the same capacity window of the cell, the resulting degradation is very different in magnitude, and perhaps in mechanism, although that will be evaluated using forthcoming data from continued testing.

Ongoing Testing

INL

Testing continues for NMC/LTO cells cycled at various rates. These cells have exhibited rather low amounts of capacity loss over several thousand cycles at various rates and temperatures. The cells cycled quickly—at 6C discharge and 1C charge—have lost a similar amount of capacity to the cells cycled at 1C discharge and 0.5C charge, at reference performance test 10. Thus, the more slowly cycled cells have exhibited much faster capacity loss, per cycle, than the cells cycled at high rate. Diagnostic analysis is planned to examine the root cause of the relatively accelerated fade in the gently cycled cells.

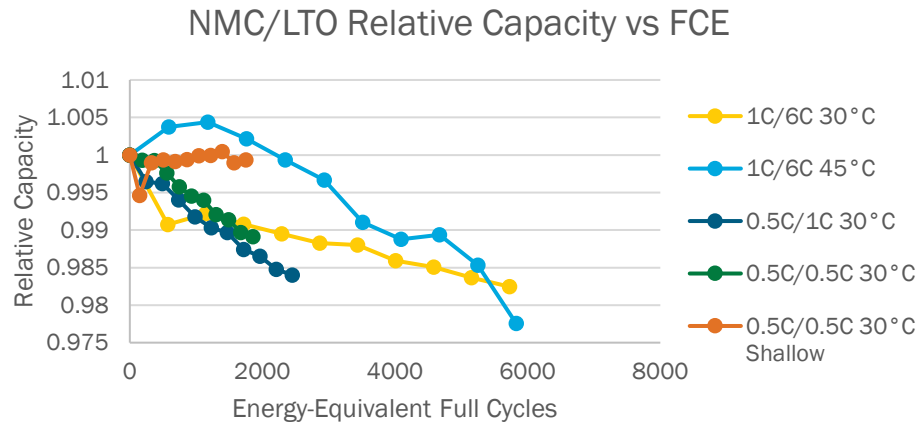


Figure 4. Cycling data for LTO-NMC cells under different charge/discharge conditions.

Upcoming Testing

Electric Applications Incorporated

Based on the test cycles discussed, EAI has selected the following lead battery types to be tested:

Conventional Lead Battery

- High-carbon AGM
- Flat-plate gel
- Thin-plate pure lead

Advanced Lead Battery

- Quasi bipolar (Dunlop Pulsar architecture)
- Bipolar (stacked-plate architecture)

The conventional lead batteries were selected to represent current technology used in reserve power and photovoltaic applications. The advanced lead batteries were chosen to represent technology that has the potential to provide better performance in grid energy storage applications. These batteries incorporate a bipolar architecture rather than the monopolar architecture used by the conventional lead batteries.

The basic monopolar architecture, as shown in Figure 4, evolved over the past century to meet specific applications for automotive starting and traction power batteries. The performance of this architecture is limited by the following key factors:

- About 40% of the lead incorporated into the battery is not electrochemically active
 - Current distribution in the cell is uneven
-

- Electrolyte tends to stratify

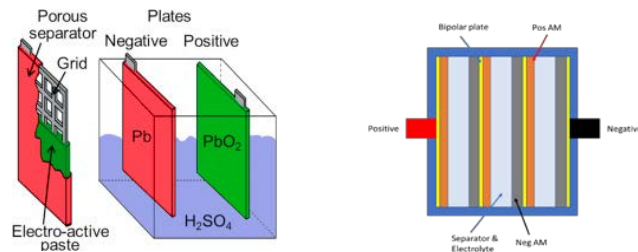


Figure 4. Monopolar architecture for a lead acid battery (left) and a bipolar architecture design (right).

The bipolar architecture is an attempt to eliminate inactive lead and provide uniform current pathways to maintain even current distribution and electrolyte concentration. It uses a single plate serving as both a positive and negative electrode. The plate is impermeable to the sulfuric acid electrolyte, but conductive to electric current. This allows one side to be prepared as a positive electrode and the other side of the plate to be prepared as a negative electrode. A multi-cell battery is then assembled by stacking the plates with a separator and electrolyte between them. Current collectors are then placed at the most positive and the most negative ends of the battery to collect the current uniformly flowing through the multiple cells of the battery.

One model of each conventional battery type and each advanced battery type will receive characterization testing. This characterization testing will allow the charge and discharge currents for each test cycle to be selected to optimize battery cycle-life. Based on the characterization testing, duplicates of two models of conventional lead batteries and duplicates of one model of advanced lead batteries will be placed in cycle-life testing using each of the two test cycles. Cycle-life testing is expected to continue throughout the next reporting period.

INL

INL has begun lab work to prepare for screening of more than 50 LMO/LTO cells to ensure that the devices tested will be initially well matched. Screening will consist of static capacity tests, rate capability tests, and quasi-OCV tests. Nickel/zinc cells were received and will be tested against the two protocols discussed above.

Summary

Aging continues for a few commercial cells that began early in the program as a benchmark, not meeting the critical-materials-free goal. New critical-materials-free commercial cells will begin testing and evaluation in July using the recently developed BTMS device-level cycling routines.

BTMS Materials Development

Yeyoung Ha, Yicheng Zhang, Sang-Don Han, Kyusung Park (NREL), Steve Trask, Shabbir Ahmed, Andrew Jansen (ANL)

Background

We developed the Behind-the-Meter Storage (BTMS) Gen1 electrolyte for $\text{Li}_4\text{Ti}_5\text{O}_{12}$ (LTO) anode and Mn-based cathode (LiMn_2O_4 (LMO) or $\text{LiNi}_{0.5}\text{Mn}_{1.5}\text{O}_4$ (LMNO)) systems, which consists of lithium hexafluorophosphate (LiPF_6) or lithium tetrafluoroborate (LiBF_4) in cyclic carbonate solvents (propylene carbonate (PC) or ethylene carbonate (EC)). In this quarter, the Gen1 electrolyte system was further studied by testing PC and EC co-solvent systems with varying EC/PC ratios. Previously, it has been shown that the ionic conductivity of electrolytes increases when EC is added to PC.¹ In addition, different salt concentrations in PC and EC systems were tested based on the LTO anode patents from Toshiba, where 2 M and 1 M salt concentration was used for EC- and PC-based electrolytes, respectively.²⁻⁴

Results

LTO and LMO electrodes tested in this report were provided by the CAMP facility at Argonne National Laboratory (ANL), and detailed information of the electrodes is listed in Table 1. LTO/LMO full cells were assembled in 2032-type coin-cell configuration using different electrolyte systems. All cells were tested at 45°C following 6 h rest at the open-circuit voltage (OCV) → 2 formation cycles at C/10 → 1000 aging cycles at 1C. Lower and upper cutoff voltages used were 1.5 and 3.0 V, respectively.

Table-1: Electrodes Examined in this Report

	Specifics
$\text{Li}_4\text{Ti}_5\text{O}_{12}$ (LTO)	- 87 wt% Samsung $\text{Li}_4\text{Ti}_5\text{O}_{12}$ + 5 wt% Timcal C45 + 8 wt% Kureha 9300 PVDF - Single-side coating on 20- μm Al foil - Coating thickness 102 μm ; Porosity 55.6%; Loading 14.20 mg/cm^2 ; Density 1.38 g/cm^3
LiMn_2O_4 (LMO)	- 90 wt% Toda LiMn_2O_4 + 5 wt% Timcal C45 + 5 wt% Solvay 5130 PVDF - Single-side coating on 20- μm Al foil - Coating thickness 76 μm ; Porosity 33.5%; Loading 18.86 mg/cm^2 ; Density 2.48 g/cm^3

Figure 1 shows the performance of LTO/LMO cells cycled in a series of EC/PC solvent mixtures (EC:PC = 0:1, 1:3, 1:1, 3:1, and 1:0 by weight) with 1 M LiPF_6 salt. Among the electrolytes tested, the 100% EC electrolyte exhibited the best performance (i.e., highest capacity retention and Coulombic efficiency). In terms of capacity retention, EC and PC mixtures showed faster capacity fade compared to the 100% EC or PC systems. However, having a higher ratio of EC in the solvent resulted in a better reaction kinetics, which is manifested in the dQ/dV plot as decreased overpotential of the EC/PC blend systems compared to that of the 100% PC electrolyte (Figure 1d). We note that although the difference in the overpotentials is relatively small within the cells tested here, the effect may become significant as we move toward thicker electrodes. The enhanced performance with higher EC ratio in the solvent may be attributed to the electrolyte properties (e.g., higher ionic conductivity with higher EC content¹) and/or the electrode/electrolyte interface properties (e.g., formation of a less resistive interfacial layer in the electrolytes with different EC/PC ratios). The effect of EC and PC on the performance of the cell, especially on each electrode, will be further examined to determine the failure mechanisms in the Gen1 electrolyte.

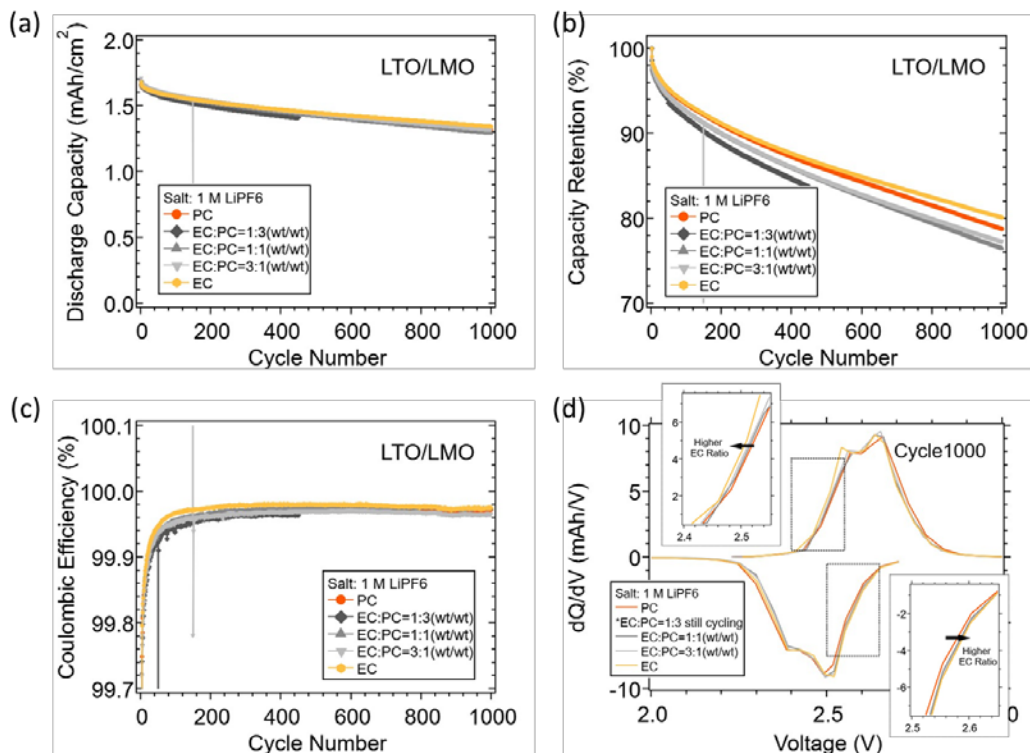


Figure 3. Cycle performance of LTO/LMO cells with 1 M LiPF₆ salt in a series of EC:PC solvent mixtures. Cells were cycled at C/10 for 2 formation cycles and at 1C for aging cycles between 1.5 and 3.0 V. (a) Discharge capacity, (b) capacity retention, and (c) Coulombic efficiency as a function of cycle number. (d) dQ/dV plot of each solvent mixture systems at the 1000th cycle.

The results of LTO/LMO cells tested with different LiPF₆ concentrations are shown in Figure 2. Previously, for the initial electrolyte development step, we fixed the salt concentration to 1 M. However, in the patents from Toshiba on the LTO electrode, 2 M LiBF₄ in EC-based solvents was used as the baseline electrolyte.²⁻³ Thus, we tested 2 M LiPF₆ in EC and PC solvents. Comparing the cycle performance, 1 M LiPF₆ in EC and 2 M LiPF₆ in EC electrolytes showed similar results. However, when using PC as the solvent, having a higher LiPF₆ concentration deteriorated the performance. Such opposite behavior in EC and PC solvents may be correlated with a higher dielectric constant of EC compared to that of PC⁵ and different solvation chemistry in the two systems. We also note that in a Toshiba patent using PC-based solvents, 1 M salt concentration was used.⁴ The dQ/dV plots of the 1st (C/10) and the 300th (1C) cycles show that the salt concentration does not affect the reaction kinetics at a lower C-rate, but it does impact the performance at a higher C-rate, especially with the PC solvent. At 1C (Figure 2d), the overpotential increases in the 2 M LiPF₆ electrolytes compared to that in the 1 M LiPF₆ electrolytes for both EC and PC solvents, but with a much greater extent in the PC solvent.

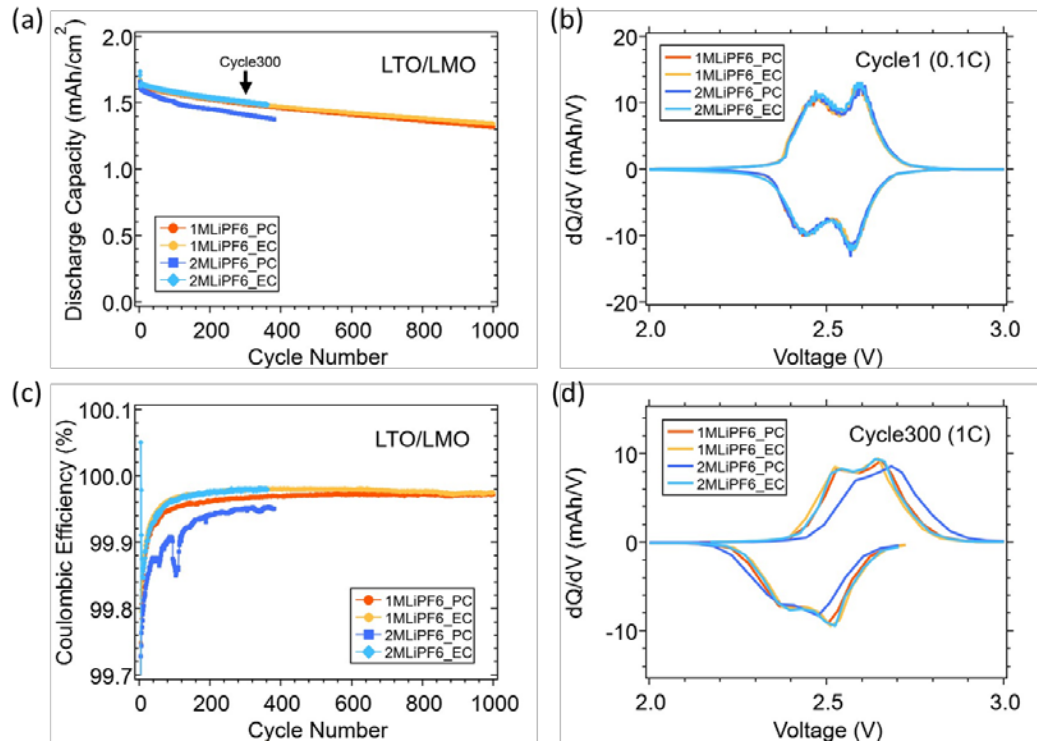


Figure 4. Cycle performance of LTO/LMO cells in electrolytes consisting of 1 M or 2 M LiPF₆ salt in EC or PC solvent. Cells were cycled at C/10 for 2 formation cycles and at 1C for aging cycles between 1.5 and 3.0 V. Discharge capacity and Coulombic efficiency are plotted as a function of cycle number in (a) and (c), respectively. dQ/dV plots of each electrolyte systems at the 1st and the 300th cycles are shown in (b) and (d), respectively.

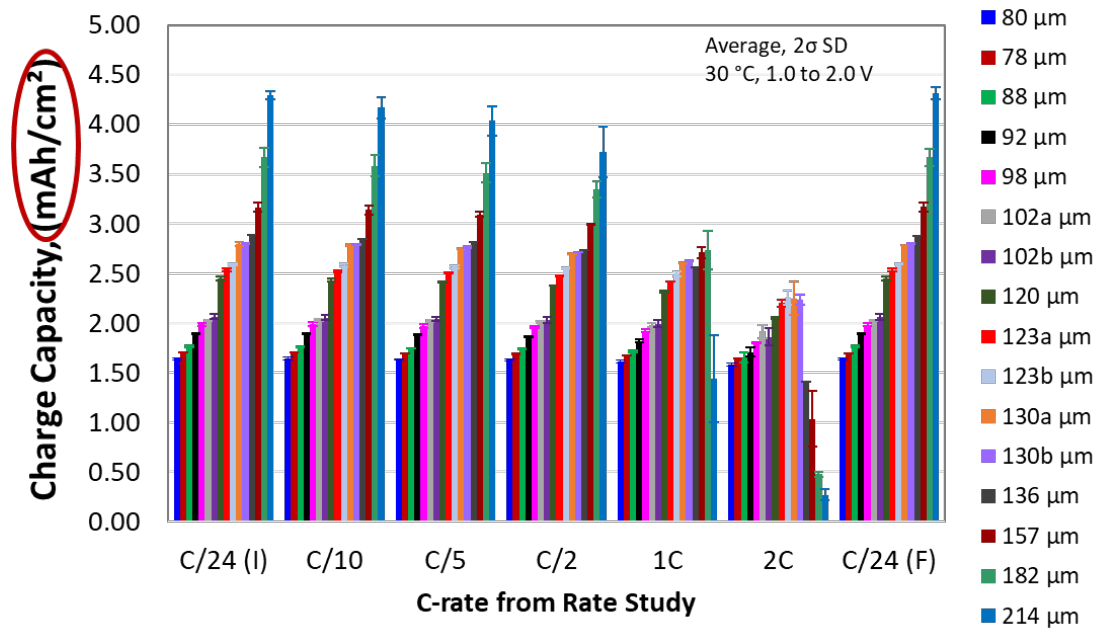


Figure 3. Capacity utilization (delithiation) as a function of electrode thickness under various delithiation rates for LTO versus lithium metal in coin cells (Gen2 electrolyte, 30°C, 1.0 to 2.0 V).

The CAMP Facility at ANL coated LTO, LFP, and LMO single-sided electrodes to test the effect of thickness (capacity/mass loading) on active material utilization. All coatings used aluminum foil as the current collector and PVDF as the binder. These electrodes were calendered (~53% for LTO, ~41% for LFP, and ~34% for LMO), where the porosity was limited due to electrode curling, which is a common problem for single-sided electrodes. The LTO and LFP electrodes were tested in coin cells versus lithium metal, with Gen2 electrolyte (1.2 M LiPF₆ in EC:EMC (3:7 by wt.)) at current rates of C/24, C/10, C/5, C/2, 1C, and 2C (LTO lithiation and LFP delithiation sub-cycles were limited to C/5). The LMO electrodes will be tested in the next quarter.

Figures 3 and 4 are a graphical summary of the capacity utilization as a function of electrode thickness for LTO and LFP, respectively. Two coin cells were tested for each thickness shown, and the resulting capacities were averaged for each current rate. It can be surmised from a study of both figures that the capacity of LTO and LFP were well utilized at all thicknesses up to a current rate of C/2. However, the capacity of LTO and LFP were not fully utilized at the 1C current rate for the thicker electrodes. In particular, the LTO electrodes above 150 microns were limited in performance. But keep in mind that the LTO electrodes had high porosity (~53%) because they were single-sided: a double-sided electrode would have lower porosity, implying the final electrode thickness may be limited to ~130 microns. The LFP electrode thickness also appears to be limited to near 130 microns. Note that these thickness limitations at high “discharge” rates may be due to lithium plating and stripping limitations at the lithium counter electrode. Full cells of LTO versus LMO with select capacity-matched thicknesses will be tested for rate capability in the next quarter.

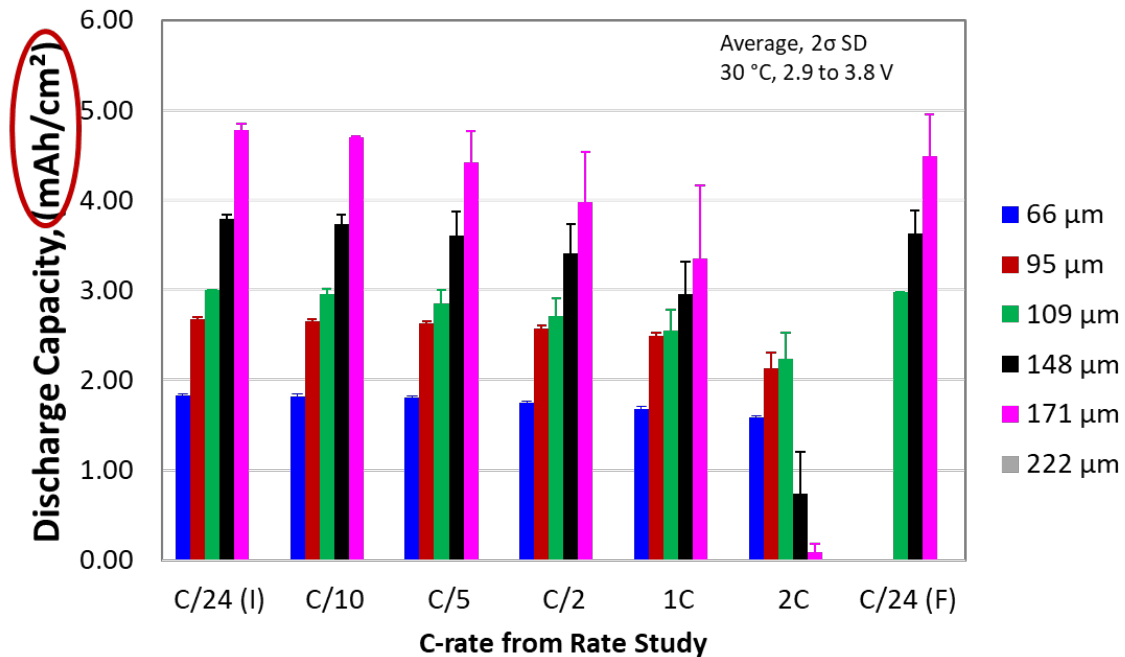


Figure 4. Capacity utilization (lithiation) as a function of electrode thickness under various lithiation rates for LFP versus lithium metal in coin cells (Gen2 electrolyte, 30°C, 2.9 to 3.8 V).

Conclusions

LTO/LMO cells were tested in LiPF₆-based electrolytes using EC and PC solvents. With varying EC/PC ratios, having a higher EC content enhanced the performance. In addition, the salt concentration (1 M vs. 2 M) did not have a critical impact on the performance when EC was used as the solvent, but a worse performance was observed at a higher salt concentration with PC. To determine the failure mechanisms in the BTMS Gen1 electrolyte, we will perform detailed electrochemical analysis using symmetric cells, which will allow us to deconvolute the different chemistries at the anode and the cathode. In addition, we will continue to explore new electrolyte systems, especially for high-voltage cathodes. Finally, thicker electrodes will be tested to determine the thickness limitations considering the specific power and specific energy at different temperatures.

In the CAMP part, we made significant progress despite the reduced lab time in this quarter due to the COVID-19 pandemic. Single-sided electrodes of LTO and LFP that were made and put on test at the end of the 2nd quarter finished cycling in the 3rd quarter, and the data were analyzed. These results are now being used in the BatPaC techno-economic model, which will be discussed in the next quarter. LMO electrodes were fabricated at the end of this quarter and will be put on test in the 4th quarter.

References

1. Ding, M.S., T.R. Jow, How Conductivities and Viscosities of PC-DEC and PC-EC Solutions of LiBF₄, LiPF₆, LiBOB, Et₄NBF₄, and Et₄NPF₆ Differ and Why. *J. Electrochem. Soc.* **2004**, *151*, A2007-A2015.
 2. Inagaki, H., N. Takami, Toshiba Corp, 2013. Nonaqueous-electrolyte battery and battery assembly. U.S. Patent 8,524,411.
 3. Inagaki, H., H. Saruwatari, Y. Fujita, N. Takami, Toshiba Corp, 2014. Nonaqueous electrolyte battery, battery pack and vehicle. U.S. Patent 8,663,850.
 4. Saruwatari, H., H. Kuriyama, S. Matsuno, D. Yamamoto, Toshiba Corp, 2014. Nonaqueous electrolyte secondary battery and battery pack. U.S. Patent Application 14/164,511.
 5. Payne, R., I.E. Theodorou, Dielectric properties and relaxation in ethylene carbonate and propylene carbonate. *J. Phys. Chem.* **1972**, *76*, 2892-2900.
-